

Effect of Post-Annealing Process on Nb-Hf Alloy Produced by Spark Plasma Sintering

Sasan Ranjbar Motlagh, Hosein Momeni* and Naser Ehsani

* h_momeni@mut.ac.ir

Received: October 2020

Revised: December 2020

Accepted: January 2021

Faculty of Material & Manufacturing Technologies, Malek Ashtar University of Technology, Iran

DOI: 10.22068/ijmse.18.1.11

Abstract: In this study, the effect of annealing treatment on microstructure and mechanical properties of the Nb-10Hf-1Ti wt.% produced by Spark Plasma Sintering (SPS) was investigated. Scanning electron microscope (SEM), optical microscopy, X-ray diffraction analysis, hardness, and uniaxial tension test were used to characterize the samples. Annealing treatment was carried out in a vacuum of 10^{-3} Pa at 1150 °C for 1, 3, 5, and 7 hours and in an argon atmosphere at 1350 °C for 5 hours. Internal oxidation and subsequent hafnium oxide formation causes the hardening of the C103 alloy and drastically increases the hardness and tensile strength. However, HfO₂ particles formed at the grain boundary cause brittleness and cleavage fracture of samples. Volume fraction, particle size, and mean inter-particle spacing of oxides significantly change by annealing which affects the mechanical properties. The SPSed sample at 1500 °C is softened by annealing at 1150 °C for 5 hours and its hardness and yield strength are reduced from 303 to 230 Hv and 538 to 490 MPa respectively. While annealing at 1350 °C for 5 hours increases hardness and yield strength increases to 343 Hv and 581 MPa respectively.

Keywords: Annealing treatment, Nb-Hf alloy, Spark plasma sintering, Internal oxidation.

1. INTRODUCTION

Niobium alloys with their high melting temperatures and low density are a good substitute for nickel-based superalloys. On the other hand, niobium has poor oxidation resistance and exhibits moderate strength at high temperatures. The addition of elements such as Ti, Hf, W, and Zr increases the strength and corrosion resistance of niobium [1]. C103 by compound Nb-10Hf-1Ti wt. % is one of the important niobium base alloys that has a good production capability. The common method of producing niobium alloys is the use of casting methods such as vacuum arc remelting [2]. The economic aspects of producing niobium alloy castings were also severely hindered by the loss of metal in the form of gates, skulls, and risers. Unlike titanium and nickel alloys, the gates and other casting scrap are not remeltable for niobium alloys due to the low tolerance for interstitial impurities [3]. Powder metallurgy can help in the production of homogeneous chemical composition and microstructures. And also provide the production of dense and close to the final piece shape [4]. Spark plasma sintering (SPS) is a new sintering method used to sinter powders under the effect of current and pressure. SPS has advantages such as application for different materials, high relative

density, short sintering time, and production of components with fine grain structures [5]. Several studies have been done on the SPS of niobium [6] and niobium alloys [7,8], and particularly on Nb-Si alloys [9-11]. The effect of SPS process parameters on the microstructure and mechanical properties of Nb-Zr alloy are investigated. The results show that by increasing sintering temperature, the densification of samples is partially increased but their hardness increased significantly due to the reduction of pores [12]. Effect of annealing heat treatment on microstructure and mechanical properties in oxide dispersion strengthened (ODS) alloys fabricated by mechanical alloying and SPS was investigated. The results showed that the microstructure evolution was hardly noticed by annealing at low temperature. Although the grain structure and the nano-oxide of the SPSed sample occur coarse after high temperature heat treatment. it still maintained a high tensile strength [13]. In another case with the same production condition, the hardness of samples decreased and the average grain size increased by increasing annealing temperature [14]. Compared to other more common materials like steel or titanium alloys, niobium alloys have high flow stresses at hot working temperatures. This can lead to very high pressures on metalworking equipment tooling.

Items like extrusion dies are typically used only once and then must be replaced due to high erosion [3]. The hot working temperature of most niobium alloys is slightly higher than their recrystallization temperature. The recrystallization temperature of most niobium alloys has been reported at 1000-1350 °C [15]. The annealing process must be performed in inert gas or a high vacuum at a pressure below 1×10^{-4} torr. The use of a vacuum is preferred because it is difficult to ensure the purity of inert gas [16]. Due to the insufficient data available on the production and annealing behavior of Nb-Hf alloys by powder metallurgy method, production of C103 alloy by SPS and the effect of post-annealing heat treatment on its microstructure and mechanical properties have been investigated.

2. EXPERIMENTAL PROCEDURE

C103 powder produced by mechanical alloying [17] was used as the raw material. The alloy powder has a roughly spherical morphology with an average particle size of 1.1 μm . The powders were placed in a graphite mold with a diameter of 15 mm and then heated at the speed of ~ 50 °C/min to 1300, 1500, and 1600 °C for 20 min under 40 MPa pressure. After the SPS process, samples were annealed in a box furnace under an argon atmosphere at 1350 °C or a tubular furnace under a vacuum of 10^{-3} Pa at 1150 °C. Annealing temperatures are selected according to the recrystallization temperature of the alloy, which is 1200 °C [2]. Table 1 shows the annealing conditions of the SPSed samples. The microstructure of samples was examined on a TSCAN – VEGA3 scanning electron microscopy (SEM), SEM studies using backscattered electron (BSE) images, and energy-dispersive X-ray spectroscopy (EDS) were conducted to reveal the phase constituents of annealed samples. XRD measurements were carried out using a PHILIPS- PW1800 machine with Cu k_{α} radiation ($k_{\alpha} = 0.1541$ nm). Phase characterization was conducted using X'PERT PRO software. To investigate the mechanical properties of the SPS and annealed samples, they were wire cut for uniaxial cold tensile test. The tensile test was performed according to ASTM E8 standard. The density of sintered and annealed samples was measured by the Archimedes' principle. As well as, the Vickers

hardness test was carried out from sintered samples before and after annealing. Vickers hardness was tested at a load of 30 kg. Average hardness values were obtained from at least five indents on each sample.

Table 1. Annealing conditions of SPSed samples.

Annealing time (hour)	Annealing temperature (°C)	SPS temperature (°C)	Furnace atmosphere
1	1150	1500	Vacuum 10^{-3} Pa
3	1150	1500	Vacuum 10^{-3} Pa
5	1150	1500	Vacuum 10^{-3} Pa
7	1150	1500	Vacuum 10^{-3} Pa
5	1350	1300	Ar (99.99%)
5	1350	1500	Ar (99.99%)
5	1350	1600	Ar (99.99%)

3. RESULTS AND DISCUSSION

Fig. 1 shows the microstructure of the sample sintered at 1500 °C before (Fig. 1(a)) and after annealing (Fig. 1(b)). SPSed samples according to the conditions given in Table 1 have been annealed at 1150 °C in different periods. The results of the EDS in Fig. 1 and XRD analysis in Fig. 2 confirmed the formation hafnium oxide.

Given that the annealing of samples is carried out in the vacuum, the source of oxygen for the formation of hafnium oxide is related to the oxygen present in the niobium, which is present as a solid solution. According to the equilibrium diagram of Nb-Hf-O [18], Nb dissolves more oxygen in its lattice as a solid solution with increasing temperature.

Also, the amount of soluble oxygen in niobium is increased with the addition of hafnium. It should be noted that Nb-Hf alloys are prone to internal oxidation during heat treatment under vacuum and oxygen pressure ranging from 5×10^{-3} to 1×10^{-1} Pa [19]. Diffraction pattern analysis of Fig. 2 shows that the hafnium oxide phase has increased slightly from 6.6 to 7.9 %wt. by annealing at 1150 °C. The formation of HfO_2 is due to the diffusion of oxygen atoms and its reaction with hafnium atoms. Internal oxidation affects mechanical properties. The deposition of

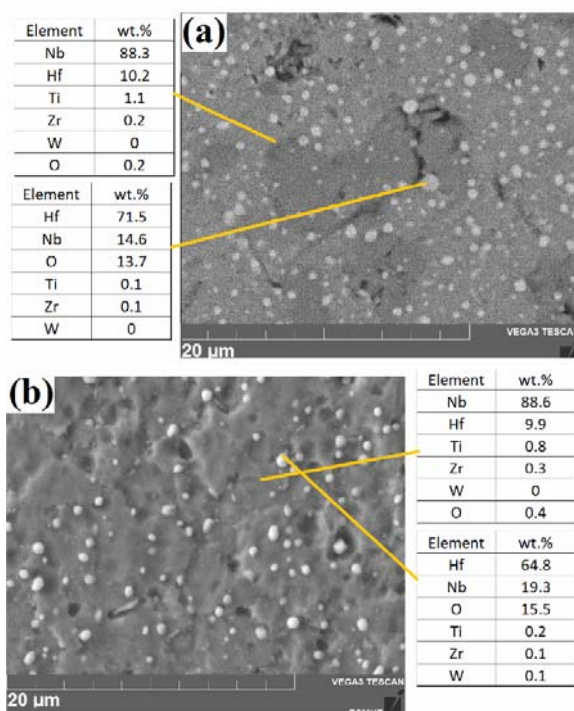


Fig. 1. SEM images of SPSed samples at 1500 °C a) before annealing, b) after annealing at 1150 °C for 5.

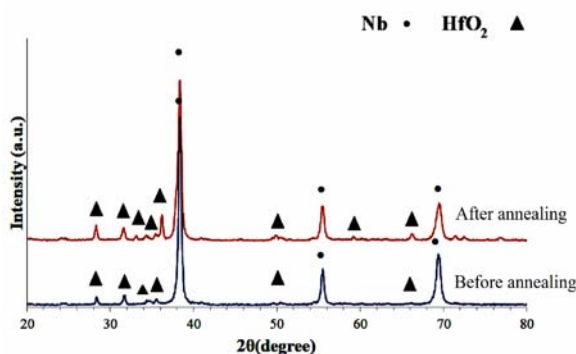


Fig. 2. XRD pattern of SPSed samples at 1500 °C before and after annealing at 1150 °C for 5.

dissolved elements can reduce the hardness by the elimination of solution hardening, or increase the hardness by dispersion hardening. Fig. 3 shows the hardness of the annealed samples at 1150 °C for different lengths of times.

Annealing at 1150 °C reduces the hardness. After 5 hours, the hardness has not changed much and has reached a constant value. Hardness results show that with the formation of HfO₂ particles during the SPS process, the hardness of samples increased compared to standard C103. The hardness of recrystallized annealed C103 is 169 Vickers [20]. Analysis of Fig. 1 shows that the annealing of the samples at

1150 °C for 5 increased the average size of the oxides from 1.51 to 1.72 μm and their volume fraction from 6.1 to 7.3%. Annealing at 1150 °C couldn't change the morphology of the oxides and remains spherical. The SPSed samples at 1300, 1500, and 1600 °C were annealed in an argon atmosphere at 1350 °C for 5. The hardness results of samples are shown in Fig. 4.

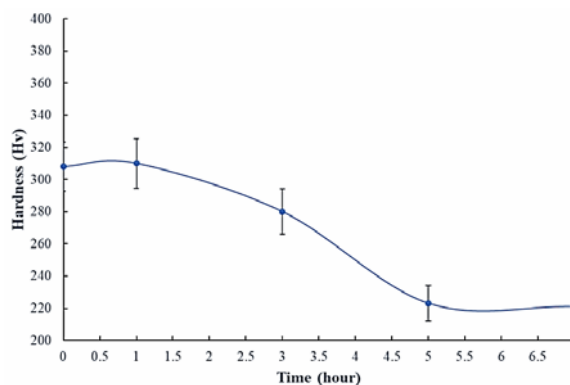


Fig. 3. The hardness curve vs annealing time of SPSed samples at 1500 °C and subsequently annealed at 1150 °C.

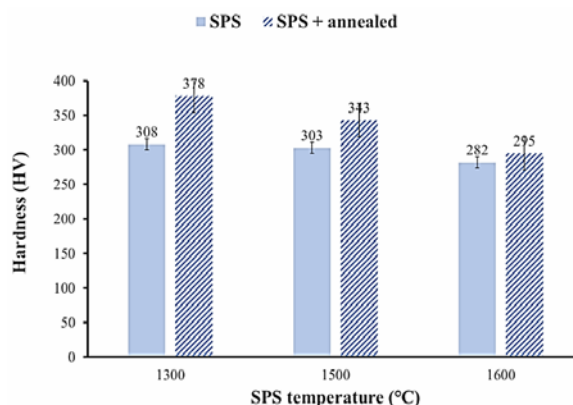


Fig. 4. The hardness of SPSed samples at different temperatures before and after annealing treatment at 1350 °C for 5.

The results of Fig. 4 show that the hardness of the specimens decreased with increasing SPS temperature. The results also indicate that by annealing, the hardness of samples has increased contrary to expectation. The hardness of the annealed samples is related to the intensification and increase of internal oxidation and some improvement of relative density. The initial relative density for specimens SPSed at 1300, 1500, and 1600 °C was 98.3, 98.1, and 97.5 % respectively. Annealing at 1350 °C for 5 improved these values to 99.7, 99.3, and 98.4 % respectively. For further study on mechanical

properties, the uniaxial cold tension test was carried out before and after annealing heat treatment. Table 2 shows the uniaxial tension test results of the SPSed samples at 1500 °C. Besides that, stress-strain curves of tensile tests are shown in Fig. 5. According to the data in Table 2, it can be concluded that the sintered samples have a good mechanical property in terms of strength but they aren't in good condition in terms of toughness. Researches on internal oxidation in other niobium base alloys have also reported this increase in strength and tangible reduction of toughness [19,21]. It should be noted that the internal oxidation of C103 produced by casting has resulted in the embrittlement of the alloy resulting in considerable lowering of strength as well as ductility [22].

Table 2. Tensile test results of SPSed at 1500 °C and annealed samples and comparison with standard.

Sample	Yield strength (MPa)	Tensile strength (MPa)	Elongation (%)
Before annealing	538	645	3.1
Annealed at 1150 °C for 1h	518	640	3.3
Annealed at 1150 °C for 5h	490	581	3.2
Annealed at 1350 °C for 5h	581	704	5.4
Standard of C103 alloy [26]	276	386	20

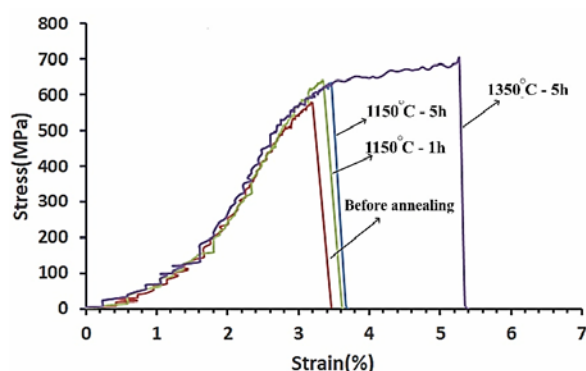


Fig. 5. Stress-Strain curves of uniaxial tensile tests of annealed samples.

The increase of yield stress may be interpreted in terms of both solid solutions strengthening of Hf and Ti and dispersion strengthening of HfO₂

particles. Thus, the increase of yield stress will be explained by the dispersion strengthening of oxide-based on the Orowan mechanism. The dispersion strengthening induced by the hafnium oxide may be caused by the Orowan strengthening mechanism, which arises due to the presence of incoherencies between the bcc matrix of Nb and the monoclinic-structured HfO₂. The HfO₂ dispersoids could enhance the strength of the alloy by preventing the movement of dislocations. Similar results have been reported in other articles on the SPS of Nb and in-situ formation of dispersoids [23]. The morphology and volume fraction of the oxides and the microstructure of the alloy have a significant effect on the mechanical properties. The formation of more hafnium oxide and increasing the nucleation and growth of them are seen in the BSE images of Fig. 6. The formation of HfO₂ is due to the diffusion of oxygen atoms and its reaction with hafnium atoms. With increasing sintering temperature, Hf and O atoms, which have not yet formed HfO₂ precipitate, diffuse through the powder particles and impart themselves to HfO₂ particles and cause the growth of them [19]. It is well known that the strengthening by dispersoids depends on volume fraction (f), size (r), and mean interparticle spacing (λ) of particles, where λ is usually expressed as a function of r and f, $\lambda = 4(1-f)r/3f$ [24]. The average size, volume fraction, and interparticle spacing of oxides before and after annealing at 1350 °C for 5 hours are given in Table 3 the distribution of oxide size in samples is also shown in Fig. 7. The results show that the annealing of the samples at 1350 °C caused the HfO₂ oxide size to increase many times. The average size of oxides was tripled and the percentage of volume fraction is up to 2 times at the SPS temperature of 1300 °C (Fig. 6(a) and (b)). In a similar study on Nb-1Zr-O, ZrO₂ particle size has tripled with increasing aging temperature from 1100 °C to 1200 °C in heat treatment.

The accelerated growth of oxide particles at 1200 °C in the alloys with excess Zr arises from the presence of free Zr controlling the speed of growth of the phase particles and from the increase of oxygen diffusivity in Nb at 1100° [2]. Here, it should be noted that the yield stress of SPSed alloys increases by more than 200 MPa with increasing HfO₂ content from 0 to 10 vol.%, while it increases by about 50 MPa with increasing HfO₂ content from 10 to 20 vol.%.

The most distinguishable difference in the microstructures between 10 and 20 vol.% for HfO₂ is in the morphology; fine spherical oxides dispersoids in the C103 SPSed at 1500 °C (Fig. 6(c)) and spherical-like and blocky oxide dispersoids in the annealed sample (Fig. 6(d)). It should be noted that the growth of hafnium oxides in the sample which was SPSed at

1600 °C, was so high that it caused the sample to crack and break in the furnace (Fig. 6(e) and (f)). The results of Fig. 7(a) show that annealing for the sample SPSed at 1300 °C causes uniformity in the distribution of oxide size. The uniformity of the oxide size is another reason for the higher hardness after annealing in the sample SPSed at 1300 °C.

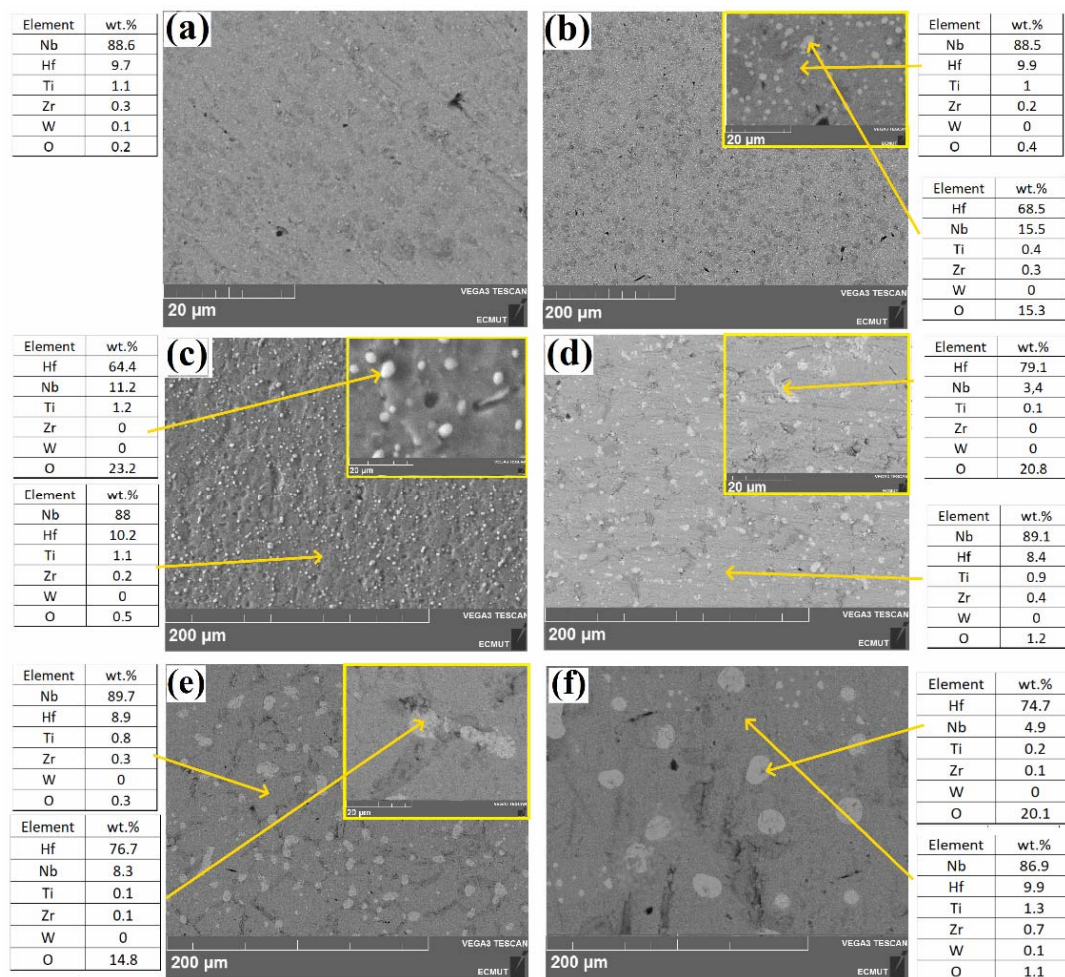


Fig. 6. BSE images of SPSed samples before and after annealing at 1350 °C for 5 respectively at different SPS temperature a, b) 1300 °C, c, d) 1500 °C and e, f) 1600 °C.

Table 3. Average particle size, volume fraction, and interparticle spacing of HfO₂ in SPSed and annealed at 1350 °C samples

SPS temperature(°C)	Average oxide size (μm)		Volume fraction %		λ, interparticle spacing (μm)	
	Before annealing	After annealing	Before annealing	After annealing	Before annealing	After annealing
1300	0.52±0.1	1.51±0.3	6.7±0.5	12.2±0.5	9.7±0.6	14.5±0.8
1500	4.55±0.7	8.4±0.5	7.1±0.8	10.5±0.6	79.4±1.5	95.5±1.3
1600	8.91±0.6	12.05±0.9	12.5±0.8	15.8±0.9	83.2±1.4	121.1±1.8

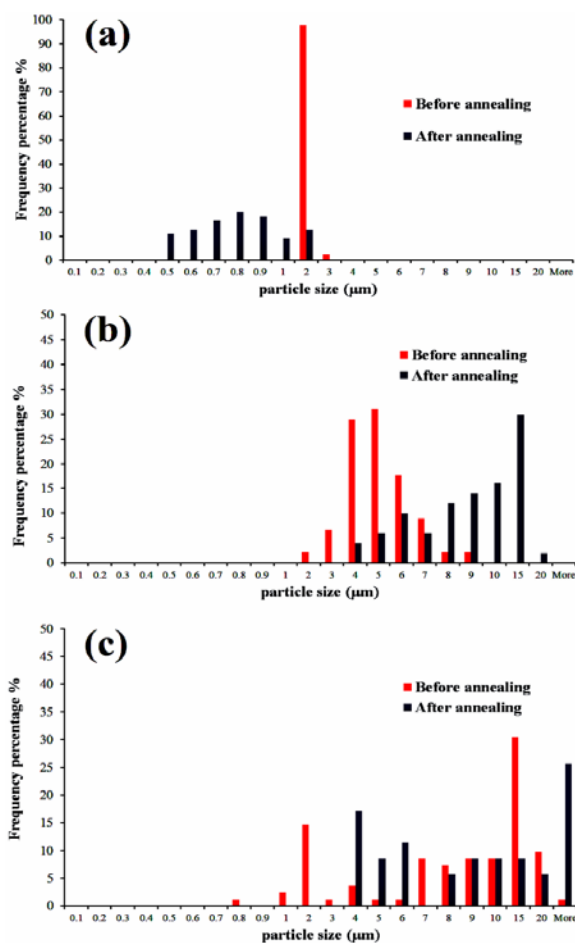


Fig. 7. Distribution of oxide size before and after annealing at 1350 °C for 5 hours at different SPS temperature a) 1300 °C, b) 1500 °C, and c) 1600 °C.

The hafnium itself is a potential source of solid solution hardening, while the HfO_2 provides dispersion hardening. By increasing the SPS temperature of the samples, the increasing trend of nucleation and growth of oxides due to annealing treatment is observed with less slope. Coarsening and increasing the distance between the oxides causes the loss of the dispersion hardening effect, which has reduced the hardness difference of the samples before and after annealing for SPSed samples at 1500 °C (Fig. 7(b)) and especially 1600 °C (Fig. 7(c)). In general, all of the alloys containing hafnium exhibited age hardening and dispersion hardening characteristics [2]. In Nb-15Hf-1.3C at. % alloy, over aging starts after 2 h at 800 °C and causes a reduction of hardness [25]. The presence of coarse precipitated hafnium oxide in the grain boundary has caused the brittleness of alloy. Fig. 8 shows the fractured surface of specimens.

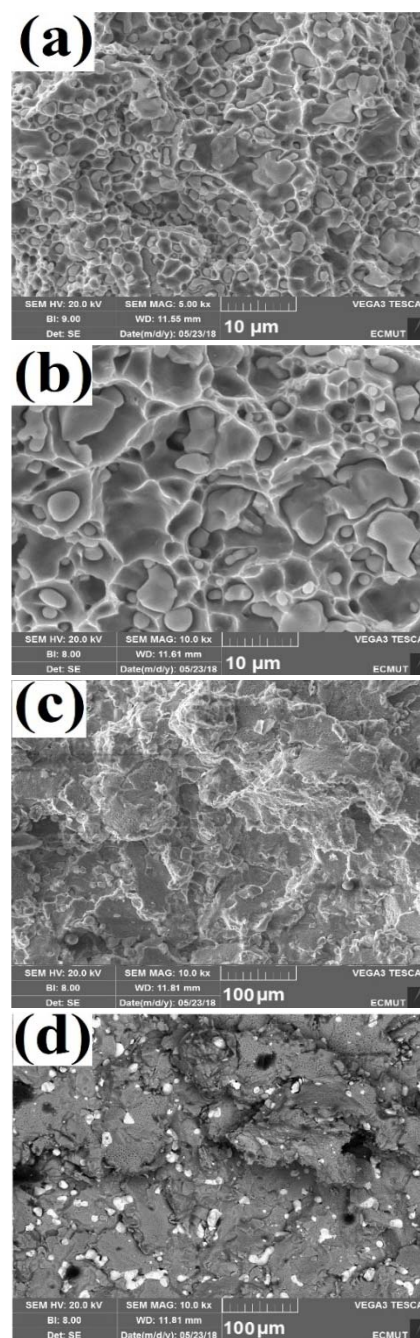


Fig. 8. SE and BSE image of the fracture surface of samples a) SPS at 1500 °C before annealing, b) SPS at 1500 °C and annealed at 1350 °C for 5, c and d) SE and BSE of SPS at 1600 °C which crack and break in the furnace during annealing.

The remarkable dispersion hardening by HfO_2 addition will reduce the plastic zone at a crack tip, thereby enhancing cleavage fracture. The river pattern is found on the fractured Nb phase (Fig. 8(a) and (b)) which illustrates that the failure manner of the Nb phase is typical of cleavage fracture. From the cleavage river

pattern direction, the crack was confirmed to initiate at the boundary of the C103 grain and propagated within the radial plane of the C103 grain in a cleavage mode. Fig. 8(c) and (d) also demonstrate that the SPSed sample at 1600 °C has coarse grains and large HfO₂ oxides with some micro holes among them. During the annealing process of the SPSed alloy at 1600 °C, the precipitated phases at the grain boundary are coarsened, which reduces the bonding force between the grain boundaries and results in the rapid development of damage and failure at the furnace during annealing of the sample.

4. CONCLUSION

In this study, the effect of annealing treatment on microstructure and mechanical properties of Nb-10Hf-1Ti wt.% produced by SPS was investigated. The results can be summarized as follows:

- Internal oxidation occurs in the alloy by the SPS process. Following that increasing in the hardness and yield strength occurred due to oxide dispersion strength. By increasing SPS temperature from 1300 to 1600 °C, HfO₂ particle size significantly grows from 0.52 to 8.9 μm.
- The temperature of the annealing treatment after the SPS process has a significant effect on the morphology, average size, volume fraction of the oxide particles. Annealing at 1150 °C has little effect on the average particle size, volume fraction, and morphology of HfO₂. While, annealing at 1350 °C has almost doubled the volume fraction, multiplied the size of the oxides, and improved the relative density of the samples.
- The SPSed sample at 1500 °C is softened by annealing at 1150 °C for 5 hours and its hardness and yield strength are reduced from 303 to 230 Hv and 538 to 490 MPa respectively. While annealing at 1350 °C for 5 increases hardness and yield strength to 343 Hv and 581 MPa respectively. In comparison with conventional C103 alloy, the hardness and yield strength are improved significantly.

REFERENCES

1. Ghosh, G., Olson, G.B., "Integrated design of Nb-based superalloys: Ab initio calculations, computational thermodynamics and kinetics, and experimental results", *Acta Mater.*, 2007,

- 55, 3281–3303.
2. Sheftel, E.N., Bannykh, O.A., "Niobium-Base alloys", *Int. J. Refract. Met. Hard Mater.*, 1994, 12, 303–314.
3. Wojcik, C.C., "Thermomechanical processing and properties of niobium alloys", in: *Niobium 2001 Int. Symp.*, 2001, 163–173.
4. Johnson, J.L., "Sintering of refractory metals", *Sinter. Adv. Mater.*, 2010, 356–388.
5. Munir, Z. a., Anselmi-Tamburini, U., Ohyanagi, M., "The effect of electric field and pressure on the synthesis and consolidation of materials: A review of the spark plasma sintering method ", *J. Mater. Sci.*, 2006, 41, 763–777.
6. Kim, Y., Lee, S., Kim, E.P., Noh, J.W., Lee, S.H., "Consolidation behavior of pure niobium powder in spark plasma sintering", *Proc. Euro Int. Powder Metall. Congr. Exhib. Euro PM 2011*, 2011, 1–4.
7. Zhang, D.Z., Qin, M.L., Zhang, L., Lu, X., Qu, X.H., "Fabrication of Nb-Based Alloy via Spark Plasma Sintering", *Adv. Mater. Res.*, 2012, 557, 38–41.
8. Murakami, T., Kitahara, A., Koga, Y., Kawahara, M., Inui, H., Yamaguchi, M., "Microstructure of Nb-Al powders consolidated by spark plasma sintering process", *Mater. Sci. Eng. A.*, 1997, 239, 672–679.
9. Goncharov, I. S., Razumov, N. G., Shamshurin, A. I., Wang, Q. S., "Effect of the Mechanical Alloying and Spark Plasma Sintering on Microstructure, Phase Composition and Chemical Elements Distribution of Nb-Si Based Composite", *Key Eng. Mater.*, 2019, 822, 617–627.
10. Xiong, B., Wang, C., Xiong, Y., Xie, D., Zhang, X., "Effects of sintering temperature on interface and mechanical properties of short carbon fiber reinforced Nb/Nb 5 Si 3 composites fabricated by spark plasma sintering", *Intermetallics*, 2019, 108, 66–71.
11. Liu, W., Fu, Y., Sha, J., "Microstructure and mechanical properties of Nb–Si alloys fabricated by spark plasma sintering", *Prog. Nat. Sci. Mater. Int.*, 2013, 23, 55–63.
12. Hussein, M.A., Suryanarayana, C., Arumugam, M.K., Al-Aqeeli, N., "Effect of sintering parameters on microstructure, mechanical properties and electrochemical behavior of Nb-Zr alloy for biomedical applications", *Mater. Des.* 2015, 83, 344–351.

13. Li, L., Chen, L., Zhang, H., Zhang, S., Zhang, Z., "Effect of annealing temperature on microstructure and mechanical properties in oxide dispersion strengthened Fe-14Cr alloys prepared by spark plasma sintering", *Mater. Res. Express.* 2019, 6, 510-516.
14. Yoshida, R., Tsuda, T., Fujiwara, H., Miyamoto, H., Ameyama, K., "Annealing effect on mechanical properties of Ti-Al alloy/pure Ti harmonic-structured composite by MM/SPS process", *IOP Conf. Ser. Mater. Sci. Eng.*, 2014, 63.
15. Savitskii, E.M., Burkhanov, G.S., "Physical Metallurgy of Refractory Metals and Alloys", Springer US, Boston, MA, 1995, 565-570.
16. Sankar, M., Reddy, Y.S., Baligidad, R.G., "Effect of different thermomechanical processing on structure and mechanical properties of electron beam melted niobium", *Trans. Indian Inst. Met.* 2009, 62, 135-139.
17. Ranjbar Motlagh, S., Momeni, H., Ehsani, N., "Effect of rotation speed and milling time to attain Nb-10Hf-1Ti alloy powders on morphology and microstructure of Nb-10Hf-1Ti powder", *Adv. Powder Technol.*, 2020, 31, 548-559.
18. Taylor, A., Doyle, N.J., "The solid-solubility of oxygen in Nb and Nb-rich, Nb-Hf, Nb-Mo and Nb-W alloys. Part II: the ternary system Nb-Hf-O", *J. Less-Common Met.*, 1967, 13, 331-337.
19. Corn, D.L., Douglass, D.L., Smith, C.A., "The internal oxidation of Nb-Hf alloys", *Oxid. Met.* 1991, 35, 139-173.
20. Chang, W., "C-103 Niobium Properties and Products", 2010, 1-27. <http://ijmse.iust.ac.ir/>
21. DiStefano, J.R., Chitwood, L.D., "Oxidation and its effects on the mechanical properties of Nb-1Zr", *J. Nucl. Mater.*, 2001, 295, 42-48.
22. Sankar, M., Baligidad, R.G., Satyanarayana, D.V.V., Gokhale, A.A., "Effect of internal oxidation on the microstructure and mechanical properties of C-103 alloy", *Mater. Sci. Eng. A.*, 2013, 574, 104-112.
23. Kang, B., Kong, T., Raza, A., Ryu, H.J., Hong, S.J., "Fabrication, microstructure and mechanical property of a novel Nb-rich refractory high-entropy alloy strengthened by in-situ formation of dispersoids", *Int. J. Refract. Met. Hard Mater.*, 2019, 81, 15-20.
24. Corti, C.W., Cotterill, P., Fitzpatrick, G.A., "The evaluation of the interparticle spacing in dispersion alloys", *Int. Metall. Rev.*, 1974, 19, 77-88.
25. Birla, N.C., Hoch, M., "The age hardening characteristics of Nb-Base alloys containing carbon and/or silicon: Part I. (Nb-15 At. Pct Hf)", *Metall. Trans. A.*, 1975, 6, 1631-1643.
26. Gerardi, S., "Properties and Selection: Nonferrous Alloys and Special-Purpose Materials", ASM International, 1990.